



# NUMERICAL ANALYSIS BY GALERKIN METHOD FOR MAGNETO HYDRODYNAMIC TWO-DIMENSIONAL VISCOUS FLOW ALONG A CONSTANT WEDGE THROUGH POROUS MEDIUM

<sup>1</sup>Pragna Lad, <sup>2</sup>Dhananjay Chauhan

<sup>1</sup> Assistant Professor, <sup>2</sup> Assistant Professor

<sup>1</sup>Shree Jayendrapuri Arts and Science College, Bharuch, Gujarat, India.

<sup>2</sup>UPL University of Sustainable Technology, Vatara, Gujarat, India.

**Abstract:** *In this paper, we have studied the boundary layer flow past a constant wedge through porous media. Here, the two-dimensional MHD flow of a viscous fluid is considered. Governing equations are transformed to a well-known Falkner-Skan type equation by using similarity transformations. Solutions in the form of velocity profiles and Skin frictions are obtained through Galerkin Method for a wide range of parameters involved*

**Key words** – Galerkin Method, Magneto Hydrodynamic Flow, Porous Media, Falkner Skan equation, Similarity transformation.

## I. INTRODUCTION

The geophysical and engineering applications are available in large variety which presents many applications of fluid flows and mass transfer problems. Example can be visibly presented from flow of chemical reactors and ground water energy storage. Fixing of small holes can be done by materials like sintered bronze or metal sheet in porous medium. If such materials are added to a region boundary of fluid flow, it is observed that the free stream velocity is continued apart from the flow and the sucked fluid is obtained at the boundary. The normal component of the relative velocity of fluid and surface of the boundary conditions is the value determined by the porosity that is represented by the normal relative velocity  $\alpha$  [3] further studied the analytical solutions through the medium of the Falkner-Skan flow, just to analyze the method of Homotopy. The magnetohydrodynamic mixed boundary layer flow through porous media along vertical flat plate are analyzed by Guedda et al.[10]. He Observed that for specific parameters multiple solutions exist.

A Homotopy analysis method was used by Xu et al.[6] to investigate the behavior of boundary layer and heat transfer in an electrically conducting incompressible viscous fluid due to impulsive stretching of the surface. This process further showed that as magnetic parameter is reducing the boundary layer thickness while the thermal boundary layer thickness is enhanced. Pavlov [9] carefully added incompressible viscous fluid into boundary layer flow by reason of deformation to an elastic surface homogeneously applied to magnetic field. Andersson [5] described that when a viscous fluid of a stretching surface is passed through a boundary layer flow of MHD then the same effect of external magnetic field was seen on the flow as the viscoelasticity. In literature, abundant papers are available to study classical MHD boundary layer flows [11],[12]. Joneidi et al.[1] has observed one decrement in boundary layer thickness while analyzing the effects of heat and mass transfer on the viscous electrically conducting fluid. Maxwell's fluid representing the two-dimensional MHD boundary layer flow through porous wall was studied by Hayat et al by using Homotopy analysis method. Exact solution for the boundary layer flow with the presence of magnetic field was delivered by Pantokratoras [2].

In this paper we study behavior of the two-dimensional magneto hydrodynamic flow of a viscous fluid over a constant wedge immersed in a porous medium. Using similarity transformations, the Falkner-Skan equation is derived from the governing nonlinear boundary layer equation, which is solved by Galerkin method using MATLAB programming for many parameters involved. Numerical results in the form dimensionless velocity profiles and skin frictions for the Hartmann number, permeability, pressure gradient and suction parameter. It is observed that the Galerkin method [4],[7] method gives a very satisfactory and accurate results.

## II. MATHEMATICAL FORMULATION

Here we consider the incompressible two-dimensional viscous MHD through porous media [13]. It is assumed that the half-space  $y > 0$  is occupied by the flowing fluids and the measurement of  $x$  - axis &  $y$  - axis are in the direction of the wedge surface and normal to the flow respectively. The viscosity effects of a large Reynolds numbers are confined with the wedge surface near field, where major role is played by viscosity and also at the far field where zero shear viscosity is important. In the presence of magnetic field  $B(x)$ , the constant wedge is completely immersed inside a porous matrix. Let we define the velocity vector  $\vec{q} = (u, v)$  with velocity components  $u$  and  $v$  are in  $x$  and  $y$  directions. When the electromagnetic field exists within the porous medium, we found some development in the velocity field. The governing equations for the two-dimensional MHD flow are given by

$$\nabla \cdot \vec{q} = 0 \quad (1)$$

$$\frac{1}{\varepsilon^2} (\vec{q} \cdot \nabla) \vec{q} = -\frac{1}{\rho} \nabla p + \frac{\mu_e}{\rho} \nabla^2 \vec{q} - \frac{\mu}{\rho K} \vec{q} + \frac{1}{\rho} \vec{J} \times \vec{B} \quad (2)$$

where  $p$  represents the pressure,  $\rho$  represents the fluid density,  $\varepsilon$  represents the porosity,  $\mu_e$  represents the effective viscosity,  $K$  represents the permeability of the porous medium and body force is represented by  $\vec{J} \times \vec{B} = \sigma (E + \vec{q} \times B) \times B$ . The Lorentz force exists due to the interaction between the magnetic field and the fluid motion. As magnetic Reynolds number is very dense hence to which the induced magnetic field is negligible. It is observed in some applications of engineering that the conductivity is not large when an externally applied field is absent. So that  $E = 0$  and hence the Lorentz force is represented by

$$\vec{J} \times \vec{B} = -\sigma B^2 \vec{q} \quad (3)$$

As a body force acted on the moving fluid only due to Magnetic drag, the right-hand side of equation (3) is multiplied by the factor  $\varepsilon^{-1}$ . Hence from (2) and (3) we obtain that

$$\frac{1}{\varepsilon^2} (\vec{q} \cdot \nabla) \vec{q} = -\frac{1}{\rho} \nabla p + \frac{\mu_e}{\rho} \nabla^2 \vec{q} - \frac{\mu}{\rho K} \vec{q} - \frac{\sigma B^2(x)}{\rho \varepsilon} \vec{q} \quad (4)$$

Outside the boundary layer,  $U(x)$  represents mainstram flow velocity in  $x$  - direction. The key idea elaborated in making the boundary layer approximation is that the effects of viscosity are dominant in the neighbouring to the surface.  $\delta$  represents the thickness of the boundary layer, with  $\delta \ll L$ , where the characteristic horizontal length is  $L$ . Therefore,  $v$  is smaller in comparison of  $u$ . Also, the elementary approximation is  $\left| \frac{\partial u}{\partial y} \right| \gg \left| \frac{\partial u}{\partial x} \right|$ .

Suppose  $\left| \frac{\partial p}{\partial y} \right| \ll \left| \frac{\partial p}{\partial x} \right|$  then equation (4) describes that the pressure  $p$  in the boundary layer is a function of  $x$  simply.

Through  $\delta \ll L$ , the term  $\frac{\partial^2 u}{\partial x^2}$  can be ignored in assessment with  $\frac{\partial^2 u}{\partial y^2}$ . By these suppositions' equivalent momentum and continuity equations are specified by

$$\frac{\partial u}{\partial x} + \frac{\partial v}{\partial y} = 0 \quad (5)$$

$$\frac{1}{\varepsilon^2} \left( u \frac{\partial u}{\partial x} + v \frac{\partial u}{\partial y} \right) = -\frac{1}{\rho} \frac{\partial p}{\partial x} + \nu \frac{\partial^2 u}{\partial y^2} - \frac{v}{K} u - \frac{\sigma B^2(x)}{\rho \varepsilon} u \quad (6)$$

$$\frac{\partial p}{\partial y} = 0 \quad (7)$$

At the edge of the boundary layer, the velocity and the mainstream flow  $U(x)$  are equal for defining the pressure distribution. Also the porous media and applied magnetic field were influenced the constant viscid flow by Bernoulli's theorem.

$$\frac{U(x)}{\varepsilon^2} \frac{dU(x)}{dx} = -\frac{1}{\rho} \frac{dp}{dx} - \frac{\mu}{\rho K} U(x) - \frac{\sigma B^2}{\rho \varepsilon} U(x) \quad (8)$$

Putting (8) in (6), the MHD boundary layer equation is obtained as

$$\frac{1}{\varepsilon^2} \left( u \frac{\partial u}{\partial x} + v \frac{\partial u}{\partial y} \right) = -\frac{1}{\varepsilon^2} U(x) \frac{dU(x)}{dx} + v \frac{\partial^2 u}{\partial y^2} - \frac{v}{K} (u - U(x)) - \frac{\sigma B^2(x)}{\rho \varepsilon} (u - U(x)) \tag{9}$$

The effects of the mainstream forcing, the viscous forces, the porous medium and the magnetic interaction on the boundary layer flow are represented by the terms on the right-hand side.  $U(x)$  is projected to follow the power-law relation  $U(x) = U_\infty x^m$ , where  $U_\infty$  is constant and  $m$  represents the strength of pressure gradient. Later on, we discussed the variations of  $m$ . The appropriate boundary conditions for the above model are given by at

$$y=0: u = 0, v = V_w \text{ as } y \rightarrow \infty: u \rightarrow U(x) \tag{10}$$

In equation (10), the condition regarding  $u$  the surface indicates that the wedge surface is inactive, and  $V_w$  represents the mass transpiration parameter. At infinity, far-away from the wedge surface, the velocity approach the mainstream flow by using the following similarity transformations.

$$\psi = \sqrt{\frac{2vxU(x)c^2}{1+m}} f(\eta) \text{ and } \eta = \sqrt{\frac{(1+m)U(x)c^2}{2\varepsilon^2 vx}} y \tag{11}$$

$$\text{where the } \psi(x, y) \text{ is defined as, } (x, y) = \left( \frac{\partial \psi}{\partial y}, -\frac{\partial \psi}{\partial x} \right) \tag{12}$$

from the system (9) to (10) we get,

$$f'''(\eta) + f(\eta)f''(\eta) + \beta(1-f'^2(\eta)) - (\Omega + M^2)(f'(\eta) - 1) = 0 \tag{13}$$

with boundary conditions

$$f(0) = \alpha, f'(0) = 0 \text{ and } f'(\infty) = 1 \tag{14}$$

### III. SOLUTION BY GALERKIN METHOD

Let consider a third order differential equation (13) with the boundary conditions (14). We take  $f(\eta)$  as before to satisfy the boundary conditions (five term solution).

$$f(\eta) = C_0 + C_1(x) + C_2(x^2) + C_3(x^3) + C_4(x^4) + C_5(x^5) \tag{15}$$

The residue is,

$$R(x) = f''' + \frac{1}{5}f - \left[ 2\beta \frac{\eta}{5} + M^2 + \Omega \right] f' + \left( \frac{\eta^2 + 10\alpha}{10} \right) f'' - \left( \frac{\eta^2 + 10\alpha}{50} \right) + (\beta + M^2 + \Omega) + \frac{\beta\eta^2}{25}$$

$$\text{We choose trail functions } \varphi_1 = \left( \frac{x^2 + 10\alpha}{10} \right), \varphi_2 = \left( \frac{x^3 + 75\alpha}{75} \right), \varphi_3 = \left( \frac{x^4 + 500\alpha}{500} \right)$$

We compute the unknown coefficients by considering the integral of the weighted residual to zero.

$$\int_0^5 \varphi_j(x) R(x) dx = 0; \quad j = 0, 1, 2, \dots, n$$

Numerical simulation is done using mathematical software, MATLAB.

**Table 1 Values of  $f''(0)$  for  $M = 1$  and Various Values of  $\beta, \Omega$  and  $\alpha$**

| M = 1    |         |                 |                |                 |                |                 |                |
|----------|---------|-----------------|----------------|-----------------|----------------|-----------------|----------------|
| $\alpha$ | $\beta$ | $\Omega = 0.1$  |                | $\Omega = 0.5$  |                | $\Omega = 1.0$  |                |
|          |         | Galerkin Method | Exact Solution | Galerkin Method | Exact Solution | Galerkin Method | Exact Solution |
| -2.5     | 0.5     | 0.5616          | 0.5540         | 0.7062          | 0.6649         | 0.7968          | 0.7946         |
|          | 1.5     | 0.9155          | 0.8627         | 1.0754          | 0.9616         | 1.0949          | 1.0736         |
|          | 2.5     | 1.2629          | 1.1399         | 1.3383          | 1.2241         | 1.3449          | 1.3274         |
| -1.5     | 0.5     | 0.7800          | 0.7768         | 0.9065          | 0.9221         | 1.0571          | 1.0530         |
|          | 1.5     | 1.2303          | 1.1470         | 1.3239          | 1.2527         | 1.4278          | 1.3848         |
|          | 2.5     | 1.6471          | 1.4605         | 1.7122          | 1.5516         | 1.6790          | 1.6608         |
| 1.5      | 0.5     | 2.4697          | 2.3886         | 2.4461          | 2.5024         | 2.5925          | 2.6361         |
|          | 1.5     | 3.0586          | 2.7601         | 2.9884          | 2.8567         | 2.9832          | 2.9704         |
|          | 2.5     | 3.0351          | 3.0754         | 3.4342          | 3.1429         | 3.2741          | 3.2614         |
| 2.5      | 0.5     | 3.2974          | 3.1865         | 3.4094          | 3.2856         | 3.5114          | 3.5006         |
|          | 1.5     | 3.4214          | 3.5184         | 3.7981          | 3.6042         | 3.7146          | 3.7052         |
|          | 2.5     | 3.9521          | 3.8064         | 3.9512          | 3.8761         | 3.9857          | 3.9730         |

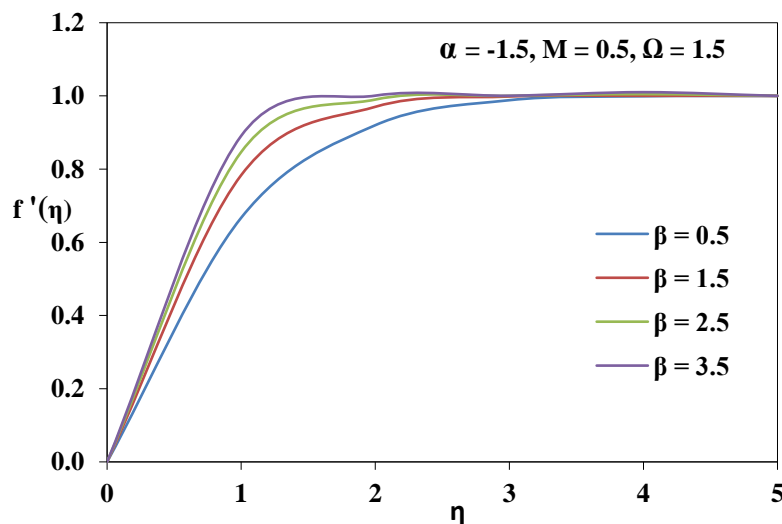
#### IV. DISCUSSION OF RESULTS

In this paper we use Galerkin method to solve the equation. The numerical results obtained for wall shear stress for three special cases, namely  $\Omega = 0.1, \Omega = 0.5$  and  $\Omega = 1.0$  are presented in Table 1. The results clearly indicates an increase in the values of wall shear stress  $f''(0)$  with increasing values of permeability parameter ( $\Omega$ ), injection parameter ( $\alpha$ ) and pressure gradient ( $\beta$ ). Some of the results from both methods are compared with the results obtained by kudenatti, Kirsur, Anchala and Bujurke.

Table 2 gives result for velocity profiles  $f'(\eta)$  for  $\beta > 0$  for fixed  $\Omega, M$  and  $\alpha$  by Galerkin Method. Fig.1 represents  $f'(\eta)$  with  $\eta$  for different values of  $\beta$  while other parameters are constant. The results obtained by Galerkin Method is included in numerically as well as graphically. The results obtained indicate the reliability of the numerical method.

**Table 2 Velocity Profiles  $f'(\eta)$  by Galerkin Method for  $\beta > 0$**

| $\eta$ | $\Omega = 1.5$ | $M = 0.5$     | $\alpha = -1.5$ |               |
|--------|----------------|---------------|-----------------|---------------|
|        | $\beta = 0.5$  | $\beta = 1.5$ | $\beta = 2.5$   | $\beta = 3.5$ |
|        | $f'(\eta)$     | $f'(\eta)$    | $f'(\eta)$      | $f'(\eta)$    |
| 0      | 0.0000         | 0.0000        | 0.0000          | 0.0000        |
| 1      | 0.6644         | 0.8382        | 0.9707          | 1.0750        |
| 2      | 1.0180         | 1.1940        | 1.3200          | 1.4160        |
| 3      | 1.1400         | 1.2310        | 1.2840          | 1.3180        |
| 4      | 1.1080         | 1.1120        | 1.0980          | 1.0800        |
| 5      | 1.0000         | 1.0000        | 1.0000          | 1.0000        |



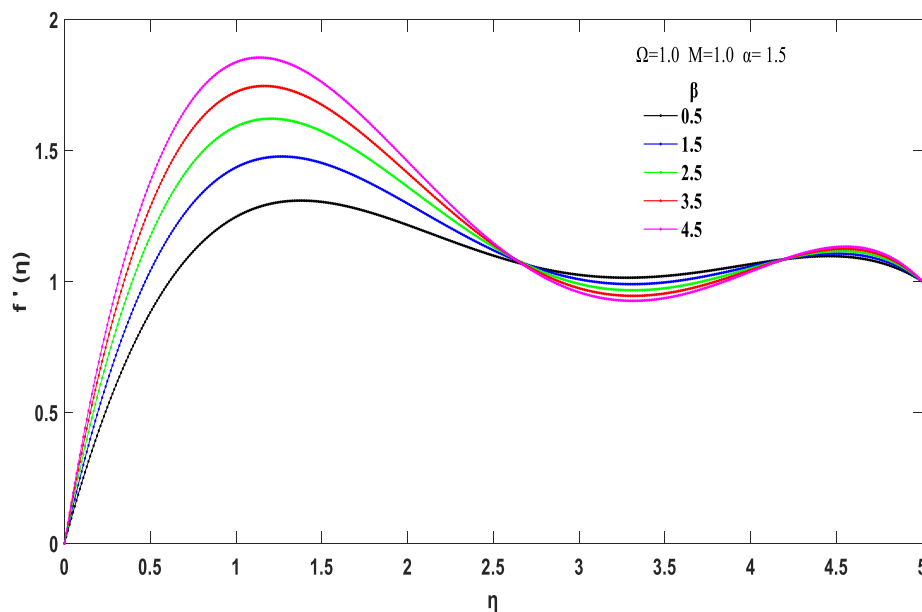
**Figure 1. Velocity Profiles  $f'(\eta)$  for  $\beta > 0$  with  $\alpha = -1.5, M = 0.5$  and  $\Omega = 1.5$  by Galerkin Method**

Table 3 gives result for velocity profiles  $f'(\eta)$  with  $\beta > 0$  for slightly fixed bigger values of other constant parameters  $\Omega, M$  and  $\alpha$  by Galerkin method. It is observed that when pressure gradient  $\beta$  is increased, the thickness of the momentum boundary layer  $[\delta = \int_0^{\infty} (1 - f'(\eta)) d\eta]$  is decreased. The same thing is plotted in fig. 2 for slightly bigger values of other constant parameters and shows that the velocity curves made the boundary layer thickness still thinner.

**Table 3. Velocity Profiles  $f'(\eta)$  by Galerkin Method for  $\beta > 0$** 

| $\eta$ | $\Omega = 1.0$ |               | $M = 1.0$     |               | $\alpha = 1.5$ |
|--------|----------------|---------------|---------------|---------------|----------------|
|        | $\beta = 4.5$  | $\beta = 3.5$ | $\beta = 2.5$ | $\beta = 1.5$ | $\beta = 0.5$  |
|        | $f'(\eta)$     | $f'(\eta)$    | $f'(\eta)$    | $f'(\eta)$    | $f'(\eta)$     |
| 0      | 0.0000         | 0.0000        | 0.0000        | 0.0000        | 0.0000         |
| 1      | 2.0280         | 1.9560        | 1.8640        | 1.7420        | 1.5730         |
| 2      | 2.2450         | 2.1830        | 2.1040        | 1.9990        | 1.8510         |
| 3      | 1.5480         | 1.5330        | 1.5130        | 1.4850        | 1.4430         |
| 4      | 0.8342         | 0.8550        | 0.8809        | 0.9136        | 0.9560         |
| 5      | 1.0000         | 1.0000        | 1.0000        | 1.0000        | 1.0000         |

The velocity profile  $f'(\eta)$  for which the solution exists, is presented in fig. 2 for  $\beta = 4.5, 3.5, 2.5, 1.5, 0.5$ ,  $\Omega = 1.0$ ,  $M = 1.0$  and  $\alpha = 1.5$  by Galerkin method. It is observed that as pressure gradient  $\beta$  increases velocity profile  $f'(\eta)$  increases.

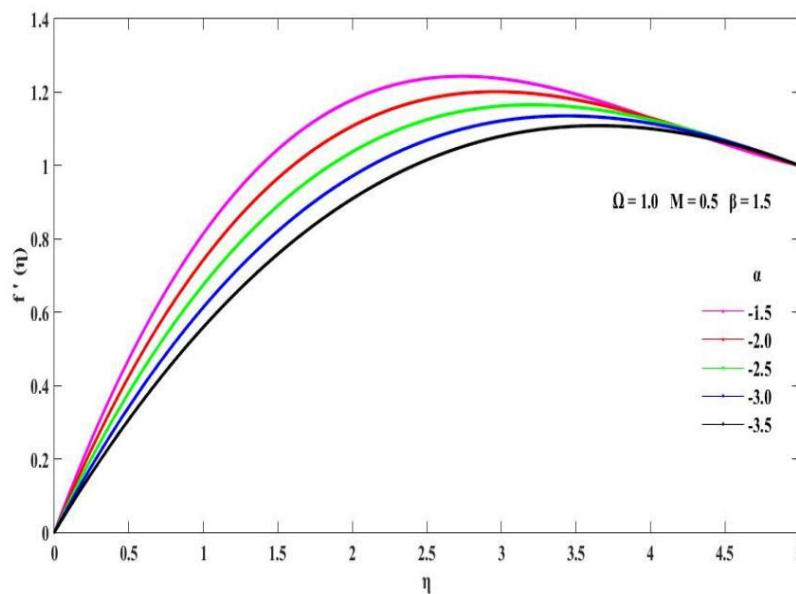


**Figure 2. Velocity profiles  $f'(\eta)$  with  $\eta$  for different value of  $\beta > 0$  for fixed  $\Omega, M$  and  $\alpha$  by Galerkin Method**

Table 4 represents the velocity profiles  $f'(\eta)$  for various value of  $\alpha$  for unchanged  $\Omega$ ,  $M$  and  $\beta$  by Galerkin method. The tabulated values indicate an insignificant difference between the solutions. In fig.3, we examine the effect of injection parameter ( $\alpha < 0$ ) when other parameters  $\Omega, M$  and  $\beta$  are constant and found that the boundary layer thickness is decreased by the mass transfer. Fig. 4, it shows that the suction parameter ( $\alpha > 0$ ) further reduces boundary layer thickness which is more prominent wherein the effect of permeability is also taken into account ( $\Omega = 2$ ).

**Table 4. Velocity Profiles  $f'(\eta)$  by Galerkin Method for  $\alpha < 0$**

| $\beta = 1.5$ |                 | $M = 0.5$       |                 |                 | $\Omega =$      |
|---------------|-----------------|-----------------|-----------------|-----------------|-----------------|
|               |                 | 1.0             |                 |                 |                 |
| $\eta$        | $\alpha = -1.5$ | $\alpha = -2.0$ | $\alpha = -2.5$ | $\alpha = -3.0$ | $\alpha = -3.5$ |
|               | $f'(\eta)$      | $f'(\eta)$      | $f'(\eta)$      | $f'(\eta)$      | $f'(\eta)$      |
| 0             | 0.0000          | 0.0000          | 0.0000          | 0.0000          | 0.0000          |
| 1             | 0.8142          | 0.7424          | 0.6747          | 0.6135          | 0.5592          |
| 2             | 1.1790          | 1.1070          | 1.0370          | 0.9710          | 0.9095          |
| 3             | 1.2370          | 1.2010          | 1.1620          | 1.1220          | 1.0800          |
| 4             | 1.1290          | 1.1300          | 1.1250          | 1.1150          | 1.1000          |
| 5             | 1.0000          | 1.0000          | 1.0000          | 1.0000          | 1.0000          |



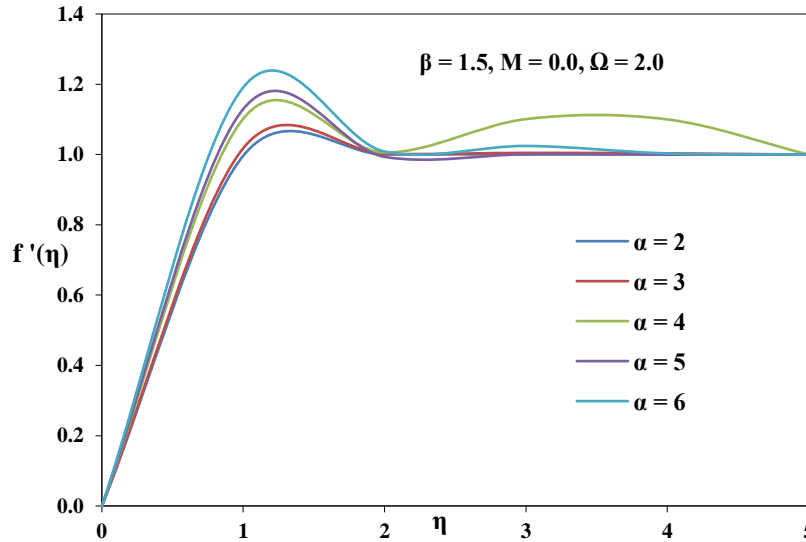
**Figure 3. Velocity Profiles  $f'(\eta)$  for Various Value of  $\alpha$  with  $\Omega = 1$ ,  $M = 0.5$  and  $\beta = 1.5$  by Galerkin Method**

Fig. 3 shows the velocity profile curves for fixed  $\Omega$ ,  $M$ ,  $\beta$  and different value of  $\alpha < 0$ . It is observed that as suction parameter  $\alpha$  increases, velocity profile  $f'(\eta)$  increases.

**Table 5. Velocity Profiles  $f'(\eta)$  by Galerkin Method for  $\alpha > 0$**

| $\beta = 1.5$ |                | $M = 0.0$      |                |                | $\Omega = 2.0$ |
|---------------|----------------|----------------|----------------|----------------|----------------|
| $\eta$        | $\alpha = 6.0$ | $\alpha = 5.0$ | $\alpha = 4.0$ | $\alpha = 3.0$ | $\alpha = 2.0$ |
|               | $f'(\eta)$     | $f'(\eta)$     | $f'(\eta)$     | $f'(\eta)$     | $f'(\eta)$     |
| 0             | 0.0000         | 0.0000         | 0.0000         | 0.0000         | 0.0000         |
| 1             | 3.5800         | 3.0090         | 2.5370         | 2.1490         | 1.8460         |
| 2             | 3.4380         | 3.0000         | 2.6310         | 2.3231         | 2.0810         |
| 3             | 1.6060         | 1.5850         | 1.5570         | 1.5242         | 1.4930         |
| 4             | 0.1158         | 0.3804         | 0.5888         | 0.7499         | 0.8697         |
| 5             | 1.0000         | 1.0000         | 1.0000         | 1.0000         | 1.0000         |

Fig. 4 shows the velocity profile curves for unchanged  $\Omega$ ,  $M$ ,  $\beta$  and dissimilar value of  $\alpha > 0$ . It is observed that as suction parameter  $\alpha$  increases, velocity profile  $f'(\eta)$  increases.



**Figure 4. Velocity Profiles  $f'(\eta)$  by Galerkin Method for Various Value of  $\alpha$  with  $\beta = 1.5$ ,  $M = 0.0$  and  $\Omega = 2.0$**

The velocity profiles  $f'(\eta)$  for different values of  $\Omega$  with fixed  $\alpha$ ,  $M$  and  $\beta$  by Galerkin method are shown in Table 6 and Table 7. For different values of permeability parameter  $\Omega$ , results interchanging has been done in fig. 5 and fig. 6 for injection shows that effect of permeability, decreases the boundary layer thickness.

When permeability increases, the boundary layer thickness decreases. And as permeability increases, the velocity profiles get closer to the thin boundary layer region, all velocity curves are confined within the thin region. Thus, the suction and permeability of the medium together have a pronounced effect on the velocity profiles.

**Table 6. Velocity Profiles  $f'(\eta)$  by Galerkin Method for Various Value of Permeability Parameter  $\Omega$  ( $\beta < 0$ )**

| $\eta$ | $\beta = -1.5$ |                | $M = 1.0$      |                | $\alpha = 1.8$ |  |
|--------|----------------|----------------|----------------|----------------|----------------|--|
|        | $\Omega = 2.5$ | $\Omega = 2.0$ | $\Omega = 1.5$ | $\Omega = 1.0$ | $\Omega = 0.5$ |  |
|        | $f'(\eta)$     | $f'(\eta)$     | $f'(\eta)$     | $f'(\eta)$     | $f'(\eta)$     |  |
| 0      | 0.0000         | 0.0000         | 0.0000         | 0.0000         | 0.0000         |  |
| 1      | 1.0740         | 1.0620         | 1.0480         | 1.0330         | 1.0320         |  |
| 2      | 1.3560         | 1.3530         | 1.3520         | 1.3540         | 1.3800         |  |
| 3      | 1.2000         | 1.2130         | 1.2320         | 1.2600         | 1.3120         |  |
| 4      | 0.9625         | 0.9823         | 1.0080         | 1.0430         | 1.0960         |  |
| 5      | 1.0000         | 1.0000         | 1.0000         | 1.0000         | 1.0000         |  |

**Table 7. Velocity Profiles  $f'(\eta)$  by Galerkin Method for Various Value of Permeability Parameter  $\Omega$  ( $\beta > 0$ )**

| $\eta$ | $\beta = 1.0$  |                | $M = 0.5$      |                | $\alpha = -1.8$ |  |
|--------|----------------|----------------|----------------|----------------|-----------------|--|
|        | $\Omega = 2.5$ | $\Omega = 2.0$ | $\Omega = 1.5$ | $\Omega = 1.0$ | $\Omega = 0.5$  |  |
|        | $f'(\eta)$     | $f'(\eta)$     | $f'(\eta)$     | $f'(\eta)$     | $f'(\eta)$      |  |
| 0      | 0.0000         | 0.0000         | 0.0000         | 0.0000         | 0.0000          |  |
| 1      | 0.7809         | 0.7527         | 0.7184         | 0.6756         | 0.6200          |  |
| 2      | 1.1250         | 1.1030         | 1.0750         | 1.0380         | 0.9857          |  |
| 3      | 1.1790         | 1.1780         | 1.1730         | 1.1620         | 1.1410          |  |
| 4      | 1.0890         | 1.1010         | 1.1140         | 1.1250         | 1.1310          |  |
| 5      | 1.0000         | 1.0000         | 1.0000         | 1.0000         | 1.0000          |  |



The behaviour of the velocity profiles  $f'(\eta)$  for different value of  $\Omega$  and for fixed  $\alpha$  ( $\alpha > 0$ ),  $M$  and  $\beta$  is shown in fig. 5

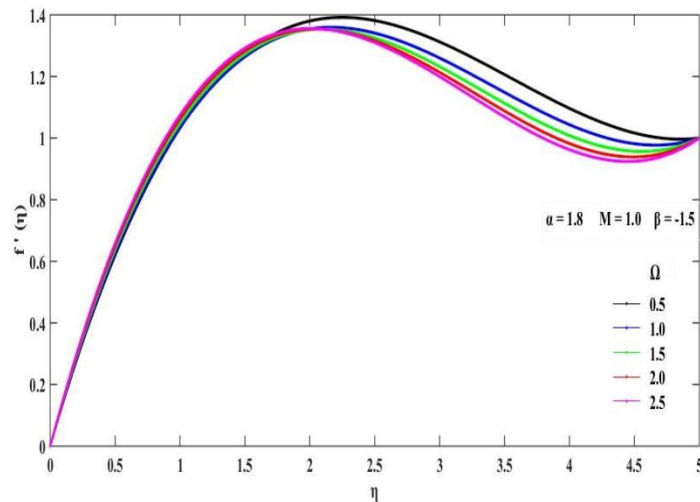


**Figure 5. Velocity Profiles  $f'(\eta)$  by Galerkin Method for Various Value of Permeability Parameter  $\Omega$  with  $\alpha = 1.8$ ,  $M = 1.0$  and  $\beta = -1.5$**

The behaviour of the velocity profiles  $f'(\eta)$  for different value of  $\Omega$  and for fixed  $\alpha$  ( $\alpha < 0$ ),  $M$  and  $\beta$  is shown in fig.6.

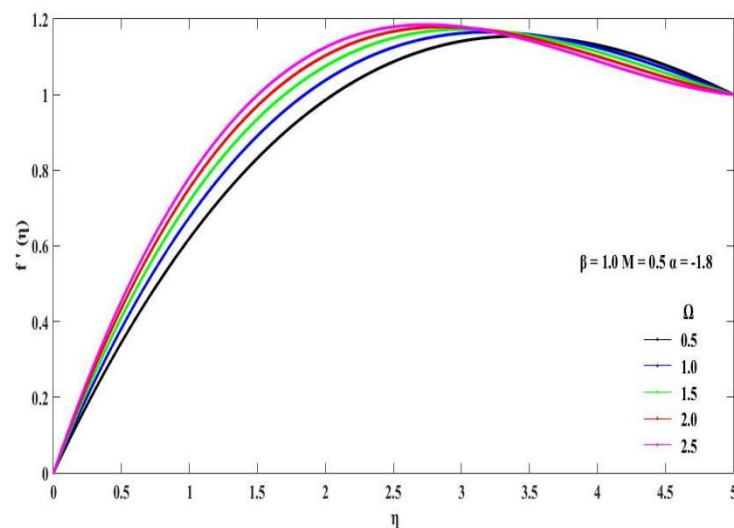


**Figure 6. Velocity Profiles  $f'(\eta)$  by Galerkin Method for Various Value of Permeability Parameter  $\Omega$  with  $\beta = 1.0$ ,  $M = 0.5$ ,  $\alpha = -1.8$**

The velocity profiles  $f'(\eta)$  for different values of  $\Omega$  and for fixed  $\alpha$ ,  $M$  and  $\beta$ , by Galerkin method is shown in fig.5 and fig. 6. Therefore, the impact of permeability is to lessen boundary layer thickness. We can see that when permeability parameter  $\Omega$  increases, the thickness of the boundary layer decreases. The numerical results obtained for wall shear stress for two special cases, namely  $\Omega = 0.3$  and  $\Omega = 1.5$  are presented in Table 8. The results clearly indicated an increase in the values of wall shear stress  $f''(0)$  with increasing values of permeability parameter ( $\Omega$ ), injection parameter ( $\alpha$ ) and pressure gradient ( $\beta$ ). All these results are in good agreement with exact solutions.



**Table 8. Wall-Shear Stress Value  $f''(0)$** 

| <b>M = 2.0</b>             |                           |                                  |                       |                                  |                       |
|----------------------------|---------------------------|----------------------------------|-----------------------|----------------------------------|-----------------------|
| <b><math>\alpha</math></b> | <b><math>\beta</math></b> | <b><math>\Omega = 0.3</math></b> |                       | <b><math>\Omega = 1.5</math></b> |                       |
|                            |                           | <b>Galerkin Method</b>           | <b>Exact Solution</b> | <b>Galerkin Method</b>           | <b>Exact Solution</b> |
| -1.5                       | 1.0                       | 1.6364                           | 1.9406                | 1.7794                           | 2.0145                |
|                            | 2.5                       | 2.0361                           | 2.4526                | 2.1299                           | 2.5148                |
|                            | 3.0                       | 2.1623                           | 2.6058                | 2.5413                           | 2.6651                |
| -1.0                       | 1.0                       | 2.1133                           | 2.1406                | 2.1485                           | 2.2156                |
|                            | 2.5                       | 2.2397                           | 2.6596                | 2.3206                           | 2.7224                |
|                            | 3.0                       | 2.3738                           | 2.8144                | 2.6384                           | 2.8744                |
| 1.0                        | 1.0                       | 2.8939                           | 3.1757                | 3.4463                           | 3.2488                |
|                            | 2.5                       | 3.1032                           | 3.6843                | 3.5141                           | 3.7462                |
|                            | 3.0                       | 3.0717                           | 3.8370                | 3.6261                           | 3.8961                |

The numerical values of velocity profiles  $f'(\eta)$  by Galerkin method for different values of permeability parameter  $\Omega$  and for fixed  $\alpha, M$  and  $\beta$  are presented in Table 9 and Table 10 are shown in fig. 7 and fig. 8 for some values of the parameter  $\Omega$  and for an adverse pressure gradient  $\beta (< 0)$ .

These results are distinct from  $\beta > 0$  which is shown in fig. 1 and fig.2. It is observed that for permeability parameter  $\Omega$ , the velocity curves oscillate finite number of times and ultimately satisfy the end condition, hence the oscillatory behaviour reveals to these solutions.

**Table 9. Velocity Profiles  $f'(\eta)$  by Galerkin Method for Various Values of Permeability Parameter  $\Omega$  with  $\alpha = -2.5$ ,  $M = 0.0$  and  $\beta = -3.0$** 

| <b><math>\eta</math></b> | <b><math>\beta = -3.0</math></b> | <b>M = 0.0</b>                   | <b><math>\alpha = -2.5</math></b> |
|--------------------------|----------------------------------|----------------------------------|-----------------------------------|
|                          | <b><math>\Omega = 2.2</math></b> | <b><math>\Omega = 1.8</math></b> | <b><math>\Omega = 1.4</math></b>  |
|                          | <b><math>f'(\eta)</math></b>     | <b><math>f'(\eta)</math></b>     | <b><math>f'(\eta)</math></b>      |
| 0                        | 0.0000                           | 0.0000                           | 0.0000                            |
| 1                        | -0.7361                          | -0.9781                          | -1.3540                           |
| 2                        | 0.6298                           | 0.3311                           | 0.0058                            |
| 3                        | 2.4570                           | 2.2290                           | 2.1430                            |
| 4                        | 3.1230                           | 3.0180                           | 3.1200                            |
| 5                        | 1.0000                           | 1.0000                           | 1.0000                            |

**Table 10. Velocity Profiles  $f'(\eta)$  by Galerkin Method for Various Values of Permeability Parameter  $\Omega$  with  $\alpha = -2.0$ ,  $M = 0.0$  and  $\beta = -4.0$**

|        | $\beta = -4.0$ | $M = 0.0$      | $\alpha = -2.0$ |                |
|--------|----------------|----------------|-----------------|----------------|
| $\eta$ | $\Omega = 1.0$ | $\Omega = 1.4$ | $\Omega = 1.8$  | $\Omega = 2.2$ |
|        | $f'(\eta)$     | $f'(\eta)$     | $f'(\eta)$      | $f'(\eta)$     |
| 0      | 0.0000         | 0.0000         | 0.0000          | 0.0000         |
| 1      | -4.3370        | -2.6650        | -1.7860         | -1.2450        |
| 2      | -2.3950        | -1.1960        | -0.5540         | -0.1444        |
| 3      | 1.8160         | 1.7050         | 1.6700          | 1.6790         |
| 4      | 4.2850         | 3.3370         | 2.8630          | 2.6020         |
| 5      | 1.0000         | 1.0000         | 1.0000          | 1.0000         |

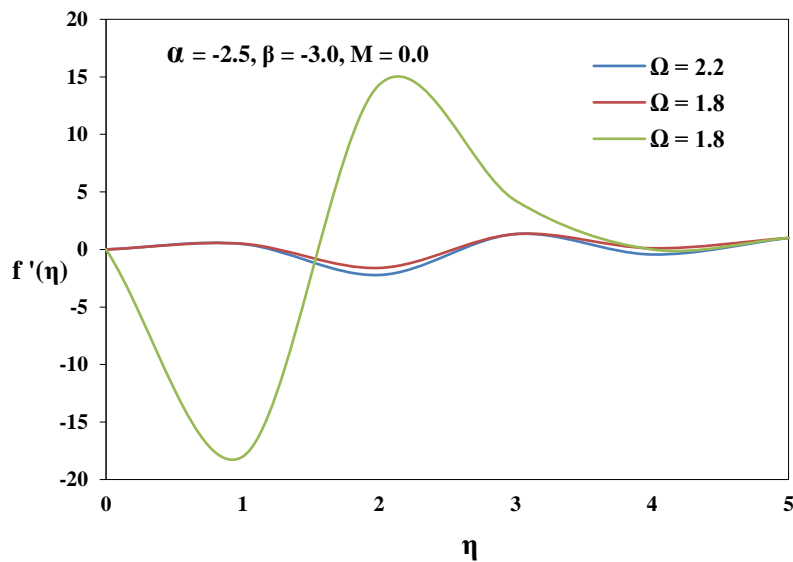


**Figure 7. Velocity Profiles  $f'(\eta)$  for Various Values of Permeability Parameter  $\Omega$  with  $\alpha = -2.5$ ,  $M = 0.0$  and  $\beta = -3.0$  by Galerkin Method**

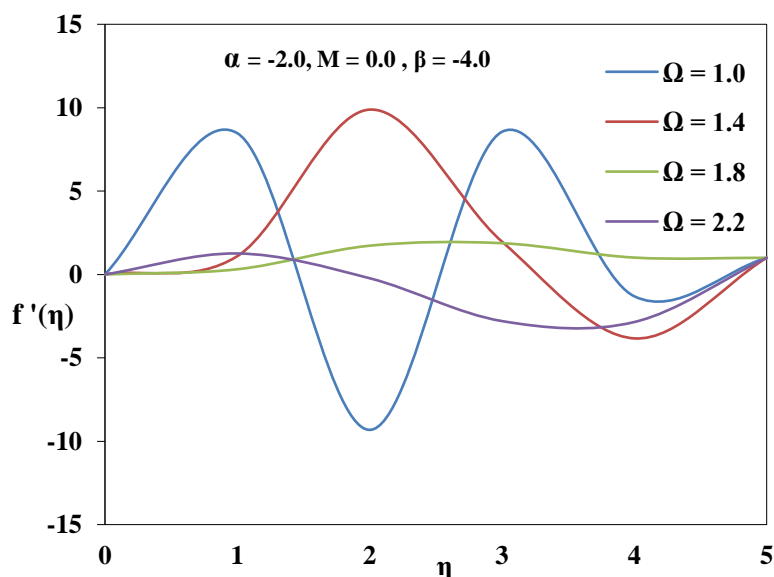


**Figure 8. Velocity Profiles  $f'(\eta)$  for Various Values of Permeability Parameter  $\Omega$  with  $\alpha = -2.0$ ,  $M = 0.0$  and  $\beta = -4.0$  by Galerkin Method**

## CONCLUSIONS

This paper illustrates a numerical simulation of the Falkner-Skan boundary layer equation using the Galerkin method. Numerical results for the velocity profile and the wall shear stress for various values of permeability parameter  $\Omega$ , injection parameter  $\alpha$ , pressure gradient  $\beta$  and  $M$  the magnetic (Hartmann number) parameters are shown in tables and graphs. Comparisons of results for certain values of parameters are made. The wall shear stress  $f''(0)$  increases with increasing values of permeability parameter ( $\Omega$ ), injection parameter ( $\alpha$ ) and pressure gradient ( $\beta$ ). When the pressure gradient  $\beta$  increase the thickness of the momentum boundary layer is decrease. The injection parameter ( $\alpha < 0$  and  $\alpha > 0$ ) when other parameters  $\Omega, M$  and  $\beta$  are held constant, we can say that the boundary layer thickness is decreased by the mass transfer. When permeability parameter  $\Omega$  increase and other parameters  $\beta, M$  and  $\alpha$  being constant then the thickness of the boundary layer is decrease. As pressure gradient  $\beta$ , permeability parameter  $\Omega$  and suction parameter  $\alpha$  increase, the velocity profile  $f'(\eta)$  increases. For  $\beta > 0$  and  $M > 0$ , the boundary layer becomes thin which is directed entirely towards the wedge surface. But if pressure gradient  $\beta (< 0)$ , the finite number of times oscillations are found for velocity curves in permeability parameter  $\Omega$ .

Another important outcome of the concerned work is the applicability of the Galerkin method which gives very satisfactory and accurate results. Hence, this chapter gives an insight to an alternate numerical method that could deal with problems of this type and if altered to perfection can provide even a better result than those obtained at present. It is also observed that when  $h$  is small, Galerkin method gives accurate results.

## REFERENCES

- [1] A. A. Joneidi, G. Domairry and M. Babaelahi, 2010 Analytical treatment of MHD free convective flow and mass transfer over a stretching sheet with chemical reaction, *Journal of the Taiwan Institute of Chemical Engineers*, 41(1) : 35–43
- [2] A. Panto kratoras, 2008. Some exact solutions of boundary layer flows along a vertical plate with buoyancy forces combined with lorentz forces under uniform suction, *Mathematical Problems in Engineering*, Article ID 149272, 1-16.
- [3] B. Yao, 2009. Approximate analytical solution to the Falkner-Skan wedge flow with the permeable wall of uniform suction”, *Communications in Nonlinear Science and Numerical Simulation*, 14 (8) : 3320–3326.
- [4] H. I. Andersson, 1992. MHD flow of a viscoelastic fluid past a stretching surface, *Acta Mechanical*, 95 (1) : 227–230.
- [5] H. Xu, S.-J. Liao, and I. Pop, 2007. Series solutions of unsteady three-dimensional MHD flow and heat transfer in the boundary layer over an impulsive stretching plate”, *European Journal of Mechanics. B. Fluids*, 26 (1) : 15–27.
- [6] K. B. Pavlov, 1974. Magnetohydrodynamic flow of an incompressible viscous fluid caused by deformation of a surface, *Magnitnaya Gidrodinamika*, 4 : 146–147
- [7] M. Guedda, E. H. Aly, and A. Ouahsine, 2011. Analytical and ChPDM analysis of MHD mixed Convection over a vertical Flat plate Embedded in a porous medium filled with water at 40°C,” *Applied Mathematical Modeling*, 35(10) : 5182–5197.
- [8] N. Chaturvedi, 1996. On MHD flow past an infinite porous plate with variable suction, *Energy conservation and management*, 37 (5) : 623-627
- [9] Ramesh B. Kudenatti, Shreenivas R. Kirsur, L.N. Achala, N.M. Bujurke, 2013 MHD boundary layer flow over a non-linear stretching boundary with suction and injection, *International Journal of non linear mechanics*, 50 : 58-67.
- [10] Riaz M., 1978. Transient Analysis of Packed-Bed Thermal Storage Systems, *Solar Energy*, 21 : 123-128.
- [11] T. Barth, P. Bochev, M. Gunzburger, and J. Shadid, 2004. A taxonomy of consistently stabilized finite element methods For the Stokes problem, *SIAM Journal on Scientific Computing*, 25(5) : 1585–1607.
- [12] T. Hayata, R. Sajjada, Z. Abbasc, M. Sajidd, and A.A. Hendie, 2011. Radiation effects on MHD flow of Maxwell fluid in a channel with porous medium, *International Journal of Heat & Mass Transfer*, 54 : 854–862.

- [13] V. A. Gradusov, V. A. Roudnev, E. A. Yarevsky, S. L. Yakovlev, 2021. Theoretical Study of Weakly Bound Triatomic Systems with Faddeev Equations in the Total Orbital Momentum Representation, *Bulletin of the Russian Academy of Sciences Physics*, 85(5) : 560-564